Multifunctional modular antenna for near-field ultra-high frequency radio frequency identification readers

Andrea Michel ✉, *Roberto Caso, Alice Buffi, Paolo Nepa*

Department of Information Engineering, University of Pisa, v. Caruso 16, 56122 Pisa, Italy

✉ *E-mail: andrea.michel@iet.unipi.it*

Abstract: A multifunctional modular antenna suitable to be embedded into low-profile ultra-high frequency radio frequency identification desktop readers is designed, prototyped and characterised at system level. Two operating modes are foreseen. The first one allows for best performance right on the reader surface (reactive near-field region), and exploits a spiral-shaped travelling wave antenna (TWA) ended on a matched load and optimised (*spiral TWA configuration*). The second operating mode exhibits a field coverage up to a few decimetres away from the reader surface (radiative near-field region), and takes advantage of the above spiral TWA that serially feeds a low-gain resonating antenna. An array of two circularly polarised miniaturised patches is here considered for the resonating antenna. By means of a switch at the spiral TWA end, each one of the two operating modes can be selected on the basis of the application scenario of interest. Specifically, the *spiral TWA configuration* is suitable for tag writing operations, when the only tag that has to be encoded is most likely placed at the reader antenna centre. On the other hand, the *modular antenna configuration* allows the desktop reader to detect tags up to few decimetres, even in presence of stacked tagged objects.

1 Introduction

In the last decade, radio frequency identification (RFID) systems have been developed and employed in several applications, such as localisation [1, 2], supply-chain or warehouse management [3], sensing [4] and item level tagging (ILT) in retail industry [5]. In the framework of ILT applications, the high-frequency RFID systems are largely applied, by providing short-range communications based on the inductive coupling between the reader antenna and the antenna of the data-provider device. However, ultra-high frequency (UHF) RFID systems are often preferred because they are able to transmit a larger amount of data in a shorter time, and smaller and cheaper tags can be used. Thus, for those applications where reader antenna and tags are in the near-field (NF) region of each other, NF UHF RFID systems have been developed. They keep the abovementioned advantages that are typical of UHF RFID systems, together with an improved robustness with respect to the effects of metals and liquids nearby the tag. NF UHF RFID systems are employed in several applications such as, for example, position sensing of small-sized laboratory animals [6], desktop readers [7–11], smart drawers, printer encoders [12], access gates, smart conveyor belts [1, 13] and smart shelves [13–15]. Consider that the antenna has to fit specific sizes and shape in order to be integrated into existing furniture or case. As an example, shelf sizes are different on the basis of the application scenario, such as in a supermarket or in a bookshelf. Also, the detection range of a NF UHF RFID antenna is ideally required to be confined to a size-limited region, to avoid cross-readings (namely false-positive readings) involving tagged items located on adjacent shelves, moving on nearby conveyors or arbitrarily placed on the desktop. Moreover, inside the above specified volume, the reader antenna has to radiate a field with an amplitude distribution as homogeneous as possible for all the field components, since the tag may be located in an arbitrary location, with any orientation. Consequently, for NF UHF RFID systems, the reader antenna represents a key element, which attracted a large interest in the recent years. Different antenna solutions have been proposed, such as segmented loops [16, 17], travelling wave antennas (TWAs) [7, 10, 11, 13, 18, 19], arrays [8, 14, 20] and oppositely directed currents antennas [21, 22, 23]. As far as desktop readers are concerned, the antenna and the low-power RFID electronics are embedded into the same case. On the contrary, in distributed RFID systems (conveyors, shelves), a reader with multiple switchable outputs is connected to a number of external different antennas that are required to guarantee satisfactory reading performance in a relatively large volume.

In most applications, the read range of a NF UHF RFID antenna is usually limited up to a few centimetres from the antenna surface. On the other hand, when the tagged objects are arranged in a pile or in bulk, tag detection must be extended up to a few decimetres. Then, it is mandatory to control both the field amplitude and the rate of its spatial decay [24] along the direction perpendicular to the reader surface as well as along directions parallel to the reader surface (when moving from the antenna centre to the borders). To extend tag readability up to a few decimetres

from the antenna surface, a *modular antenna* concept has been proposed by the authors in [25]. The modular antenna comprises a TWA and a low-gain resonating antenna, which are combined to properly shape the radiated field in both the reactive and radiative NF regions of the antenna. It is worth noting that the antenna far-field gain has to be as small as possible to avoid cross-reading issues outside the reader interrogation volume.

NF coupling phenomena are much more complex than the coupling arising when the tag is in the far-field region of the reader antenna. Then, a NF UHF RFID system cannot be characterised by means of typical antenna far-field parameter appearing in the Friis equation (e.g. radiation pattern, gain, polarisation mismatching coefficient) as it happens in conventional communication systems [26, 27]. Also, the simulated reader NF radiation alone is not effective for tag readability prediction, regardless for some specific tag layouts (i.e. small loop-like tags). For such a reason, efforts have been made to predict the tag readability on the basis of the numerical analysis of higher order coupling models where both reader and tag antennas are considered, sometimes also including the tagged item or other objects nearby the antennas [28–31]. Unquestionably, even though it could be time consuming, to date a measurement campaign is the most reliable method to assess the NF system performance in terms of power transfer efficiency [30–33], reading and writing capabilities. In particular, detection of both single tags and stacks of tags is important for a practical use of the system. Also, tests on writing operations are important too, as writing operations require a higher interrogation field amplitude with respect to the reading operations.

In this paper, a specific layout implementing the *modular antenna* concept first presented in [9] is selected and described in Section 2, together with simulated and measured antenna performance in terms of reflection coefficient and NF distributions. Specifically, thanks to its modularity, the considered antenna is able to perform in two operating modes. The performed tests, on both tag reading and writing capabilities, are focused to analyse the system-level properties of a NF UHF RFID system. Results of reading and writing tests are presented in Section 3, to assess the actual system performance.

2 Antenna layout and performance

The multifunctional modular antenna for NF FCC (Federal Communication Commision) UHF RFID (902–928 MHz) readers presented here represents an effective implementation of the *modular antenna* concept first presented in [9]. Specifically, a 50 Ω coaxial cable, placed close to the antenna centre, feeds a spiral-shaped microstrip TWA printed on a grounded 1.6 mm-thick FR4 dielectric substrate (ε_r = 4.4, tanδ = 0.025). By means of a switch, the TWA can be series connected to either a planar array of two miniaturised circularly polarised (CP) square patches (Fig. 1*a*, *modular antenna configuration*) or a matched load (Fig. 1*b*, *spiral TWA configuration*). An ideal switch has been considered in the numerical simulations, without taking into account insertion or isolation losses. In detail, for the *modular antenna configuration* the spiral TWA is directly connected to the patch array through a 3 dB power divider (Fig. 1*a*). On the other hand, for the *spiral TWA configuration* the TWA is ended on a 50 Ω resistor (Fig. 1*b*). It is worth noting that the replacement of that switch with a variable power divider would allow for a further degree of freedom to dynamically size and shape the reader detection volume, in addition to the power control that is already available in any commercial reader. For the whole antenna size, a maximum area of 275 mm × 135 mm has been assumed.

The spiral-shaped TWA overall length slightly affects the system performance since, in the *modular antenna configuration*, the spiral performs as a lossy transmission line feeding the resonating antenna. That is, if it is ended on a matched load, a stationary (non-uniform) current distribution as well as low-field minima are avoided on the antenna surface. The current distribution on the antenna surface is shown in Fig. 2. It is clear that a uniform current distribution is obtained on the spiral TWA, for both the *modular antenna configuration* (Fig. 2*a*) and the *spiral TWA configuration* (Fig. 2*b*). It is worth noting that the transmission line shape can be arbitrarily selected on the basis of the specific desktop reader size and shape. For example, a square spiral can be preferred to a circular spiral. In this case, the circular spiral line has been chosen in order to avoid the excitation of a dominant field component, making the tag detection almost independent on the particular tag orientation. Since the transmission line is directly connected to the RFID reader, the microstrip line width (W_1) has been set to 3 mm in order to get a 50 Ω characteristic impedance (W_1 has been calculated considering an 1.53 mm-thick FR-4 substrate with ε_r =and tanδ = 0.02).

A distance equal to 4.8 mm between the spiral lines is effective to minimise the effects of the coupling on the TWA input impedance. It is worth noting that in the *modular antenna configuration* the resonating antenna is fed through the TWA (that is directly connected to the reader circuit output on the other side) allowing to get a large impedance bandwidth (a −10 dB bandwidth >14%). Specifically, the spiral 50 Ω microstrip line has been connected to two 100 Ω microstrip lines (W_2 = 0.65 mm) by means of a 3 dB power divider. Each line is then connected to a miniaturised patch placed close to the spiral TWA. Since most of the reader surface must be used to accommodate the TWA antenna, six turns of the spiral TWA have been considered in the present layout, which allows the spiral to occupy the whole antenna central area. Then, a miniaturised layout is used to realise a resonating antenna that can occupy the room available at the antenna borders. Above antenna spatial arrangement, together with the will to have a

symmetric radiation in the near-field region, suggested us to employ an array of two miniaturised CP patches as a resonating antenna.

The two patches share four cuts at their corners in order to decrease patch resonance frequency (so reducing the patch surface area of about 30% with respect to a conventional patch antenna resonating at the same frequency [34]). Moreover, the length of the patch cuts is asymmetric (C = 6.2 mm, D = 2.4 mm) to excite the two quasi-degenerate modes that allow for the radiation of a CP field [35]. The main geometrical parameters values are listed in Table 1.

To summarise, given an assigned maximum antenna size, the following design procedure and optimisation parameters have been taken into account:

i. A TWA has been placed at the centre of the reader surface to improve writing capability (tags are commonly placed in proximity of the antenna centre) and to obtain best performance right on the reader surface (reactive NF region).
ii. To avoid the excitation of a dominant field component and make the tag detection almost independent on the tag orientation, a spiral-shaped travelling wave antenna has been designed. For such an element, the distance between the microstrip lines has to be properly chosen in order to limit the reflection coefficient variations (a small distance between the spiral lines leads to impedance matching issues due to the mutual coupling).
iii. A resonating antenna has been series connected to the TWA in order to detect tag up to a few decimetres, even in presence of stacks (where a stronger field intensity is needed to compensate for the mutual coupling effects between tags).
iv. The resonating antenna is designed close to the antenna borders, possibly miniaturised in order to reduce the occupied area. The miniaturisation also helps to meet the low far-field gain requirement. The resonating elements must be placed adequately far from the TWA, to limit the mutual coupling between them. In particular, in the proposed layout, two miniaturised CP patches have been considered.
v. The orientation and layouts of the two antenna modules have to be chosen by considering that the mutual coupling between the radiators sharing the reader surface is not negligible, since the radiating elements are very close to each other and they must operate at the same frequency.

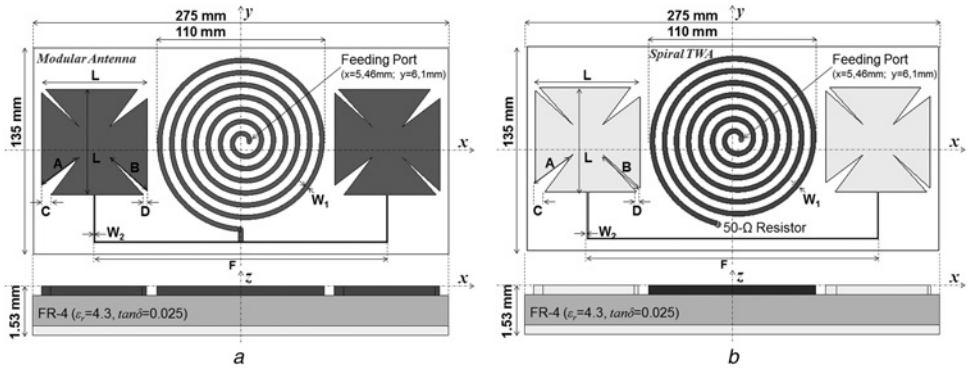

Fig. 1 *Top and lateral views of the proposed NF antennas for UHF RFID desktop reader applications. For each configuration, the active radiating elements are denoted by a light colour. The main geometrical parameter values are listed in Table 1, for an FCC UHF RFID band (902–928 MHz) reader*
a Modular antenna configuration
b Spiral TWA configuration

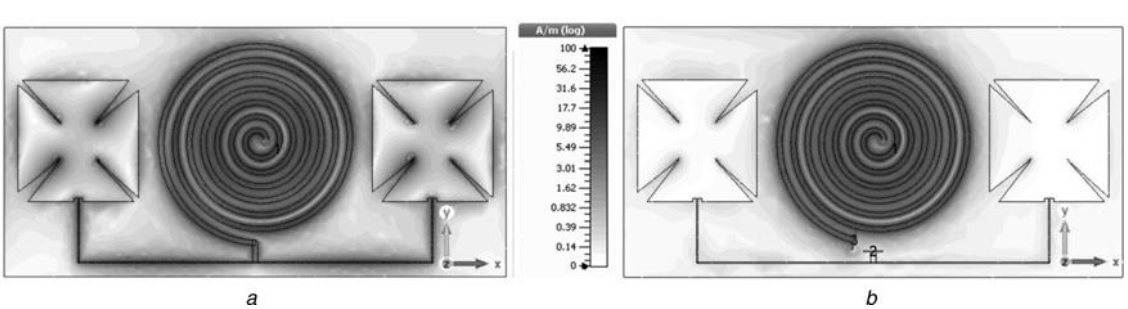

Fig. 2 *Current distribution at the frequency of 915 MHz on the antenna surface for both the antenna configurations*
a Modular antenna configuration
b Spiral TWA configuration

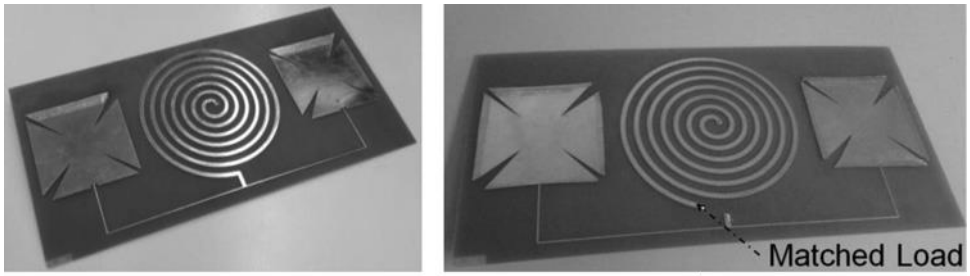

Fig. 3 *Prototype of the modular antenna for the FCC UHF RFID band*
a Modular antenna configuration
b Spiral TWA configuration

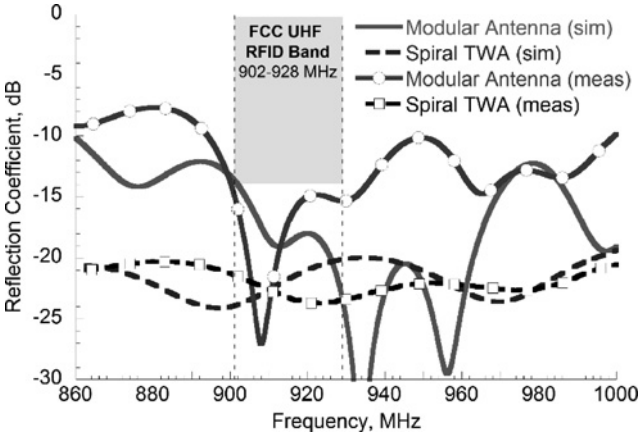

Fig. 4 *Simulated and measured reflection coefficient versus frequency for the modular antenna configuration (solid line) and the spiral TWA configuration (dashed line), in the UHF RFID FCC band*

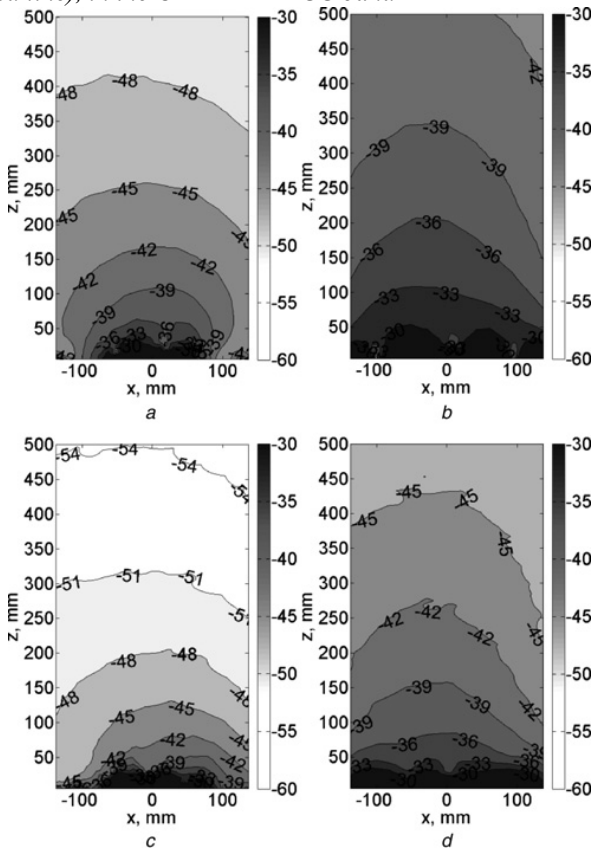

Fig. 5 *Normalised electric and magnetic field distributions evaluated on the plane orthogonal to the antenna surface (y = 0) and f_0 = 915 MHz*
a Spiral TWA configuration electric field (dB)
b Modular antenna configuration electric field (dB)
c Spiral TWA configuration magnetic field (dB)
d Modular antenna configuration magnetic field (dB)

The normalisation value is the maximum field value among the two configurations

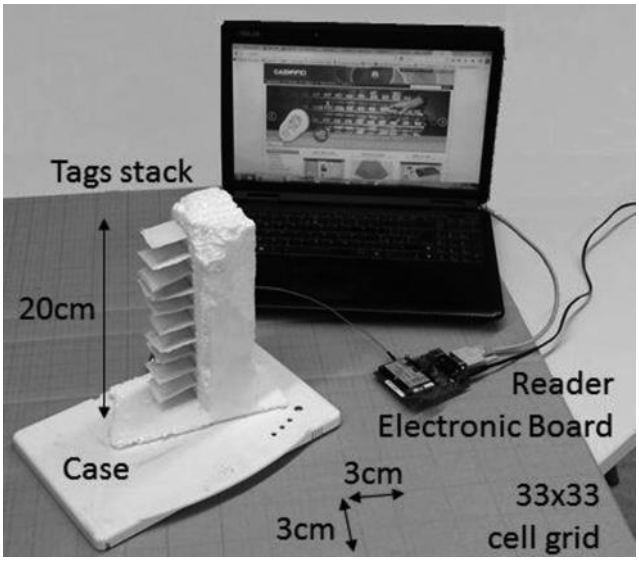

Fig. 6 *Measurement setup*

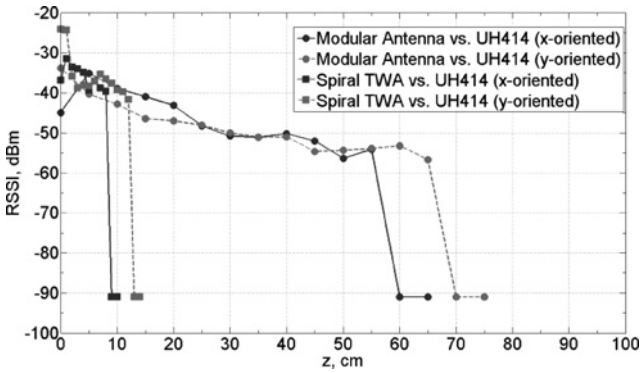

Fig. 8 *RSSI distribution by varying the tag (LABID UH414) distance from the antenna centre (along a direction perpendicular to the reader surface), with an input power of 23 dBm, for two orthogonal tag orientations and for both antenna configurations*

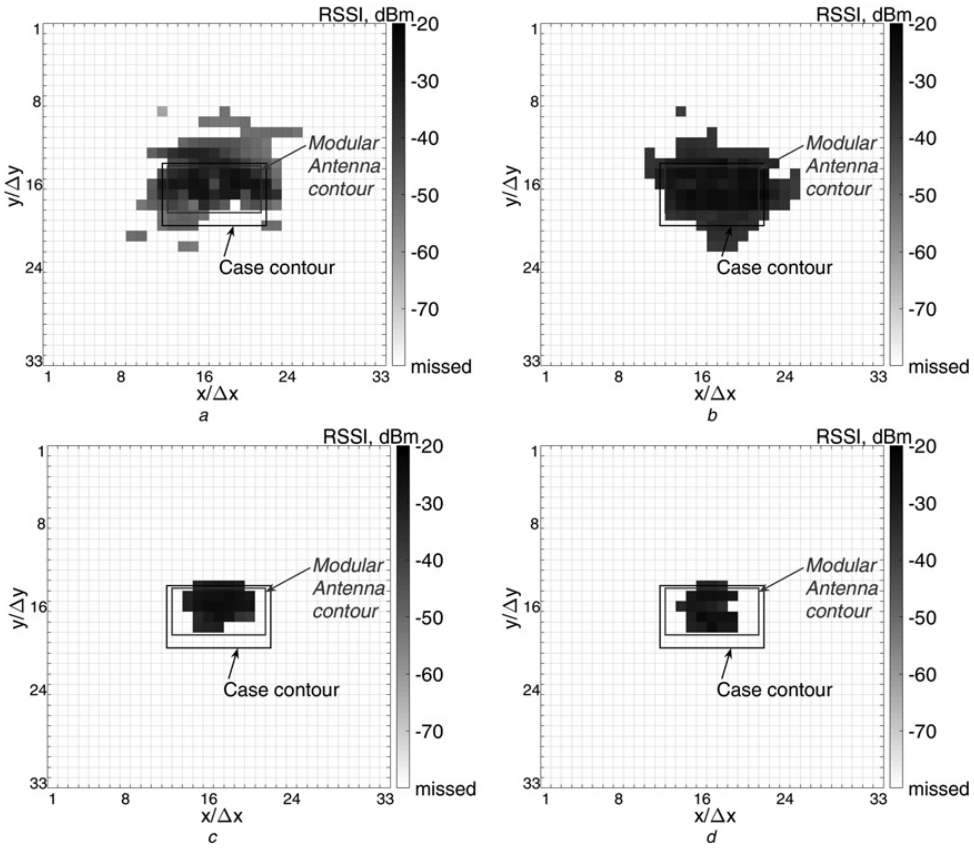

Fig. 7 *RSSI distributions on 1 m² plane parallel to the desktop reader surface (33 × 33 square cells with Δx= Δy = 3 cm), by using a LABID UH414 tag and a reader output power of 23 dBm. The following reader antenna-tag configurations have been considered*

a Modular antenna at *x*-oriented UH414 *b* Modular antenna at *y*-oriented UH414 *c* Spiral TWA at *x*-oriented UH414 *d* Spiral TWA at *y*-oriented UH414

Table 1 Antenna dimensions for UHF RFID FCC band readers Parameter Value, mm

A	31
B	33.4
C	6.2
D	2.4
F	194
L	69.7
W_1	3
W_2	0.65

For the sake of simplicity, two different prototypes have been fabricated: one for the *modular antenna configuration* (see a photo in Fig. 3*a*) and one for the *spiral TWA configuration* (see a photo in Fig. 3*b*). Such prototypes are relevant to the two operating modes achieved by using an ideal switch at the end of the TWA. The simulated and measured reflection coefficient (Fig. 4) is below −14 dB in a frequency range that is much larger than the UHF RFID FCC band (902–928 MHz), for both the *modular antenna configuration* (solid line) and the *spiral TWA configuration* (dashed line). Differences in the simulated and measured curves are mainly due to the tolerances in the substrate parameters. CST Microwave Studio® has been used to perform the simulated analysis. It is worth noting that the patch array is present in both prototypes (even if the array is disconnected in the *spiral TWA configuration*), to keep accounting for the effect of the mutual coupling between the spiral TWA and the patches. Furthermore, as shown in [9] for the UHF RFID ETSI (European Telecommunications Standards Institute) band (865–868 MHz), the far-field gain of the *spiral TWA* (when the latter is closed on a matched load) is very low (about −14 dBi from simulated results). Such a low value advises that a TWA ended on a matched load cannot be used alone if a reading range more than a few centimetres is required. On the other hand, the broadside gain of the modular antenna is about −5 dBi at the UHF RFID FCC band central frequency (i.e. 915 MHz). At the lower (902 MHz) and upper (928 MHz) frequency of the UHF RFID FCC band, the realised gain is −4.8 and −7.3 dBi, respectively. Such a value accounts for both the array gain and the TWA insertion loss. It is large enough to allow tag detection in the antenna radiative NF region, yet minimising false-positive events outside the required detection volume. Since both dipole-like tags and loop-like tags can be employed in NF UHF RFID systems, it is important to

analyse both the electric and the magnetic NF distributions (Fig. 5). The *spiral TWA configuration* exhibits a field amplitude which significantly reduces close to the reader borders and away from the surface (Figs. 5*a*–*c*), so confirming the expected rapid amplitude spatial decay (i.e. confined electromagnetic field). On the other hand, the *modular antenna* radiates a field whose amplitude decreases more slowly (Figs. 5*b*–*d*), as it is required when multiple tagged items are stacked on the reader surface.

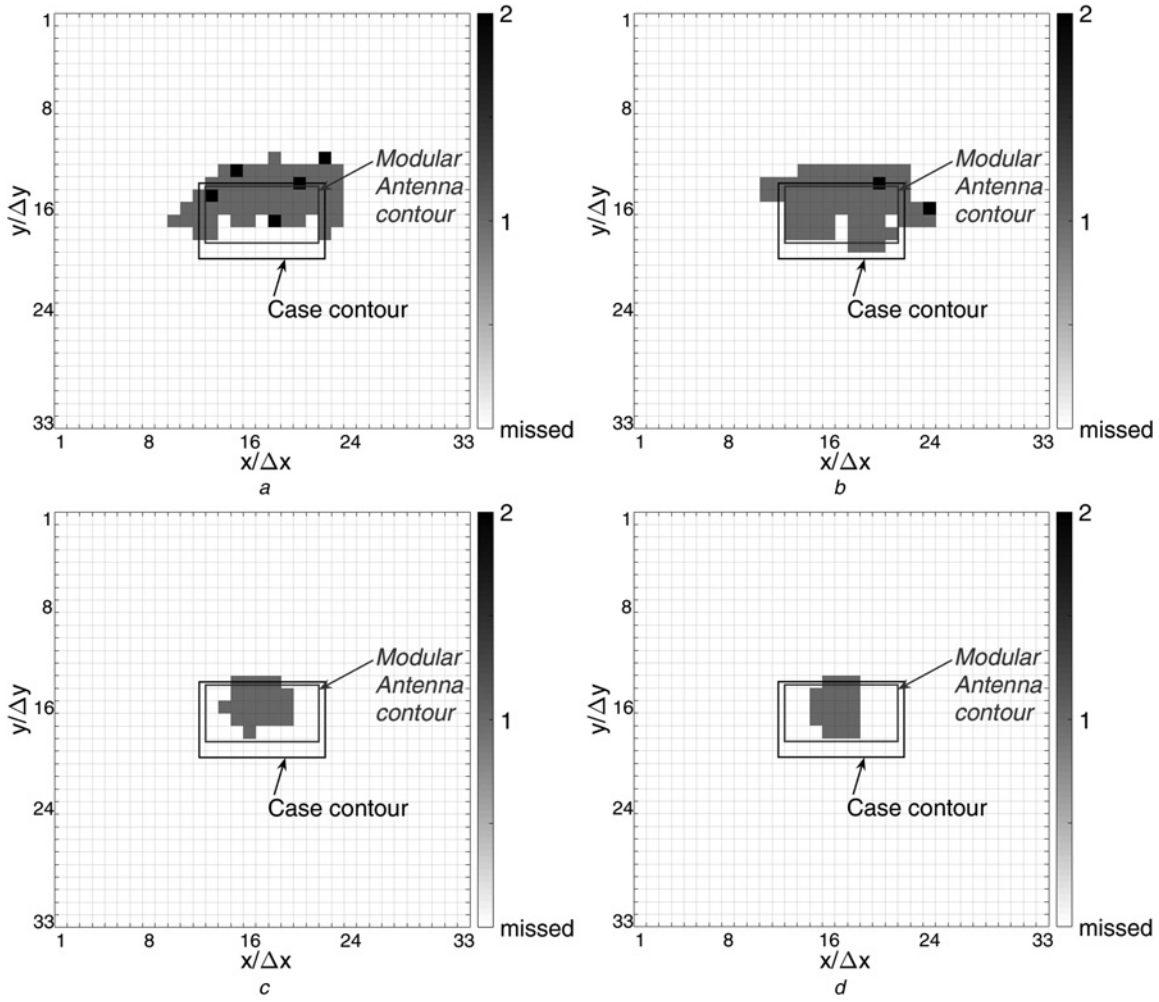

Fig. 9 *Number of attempts of writing operations on a 1 m² plane parallel to the desktop reader surface (33 × 33 square cells with Δx= Δy = 3 cm), by using a LABID UH414 tag and a reader output power of 23 dBm. The following reader antenna-tag configurations have been considered*
a Modular antenna at *x*-oriented UH414 *b* Modular antenna at *y*-oriented UH414 *c* Spiral TWA at *x*-oriented UH414
d Spiral TWA at *y*-oriented UH414

3 Antenna reading/writing performance

The antenna prototypes have been integrated into a desktop reader case (30 cm × 18 cm) and connected to the reader module A528 from the CAEN RFID company [36] (http://www.caenrfid.it/en/). Tests have been performed by using by using compact-dipole UH414 tags from the LABID company [37] (http://www.lab-id.com/datasheet/inlay_UHF/UH414.pdf). The measurement setup is shown in Fig. 6. The reader output power has been set at 23 dBm. In the software tool provided by CAEN RFID together with the UHF fixed reader, the provided received signal strength indicator (RSSI) value represents the amplitude of the signal backscattered and received at the reader input port. The reader sensitivity is −70 dBm.

3.1 *Reading/writing tests for a single tag*

During the measurements, the desktop reader was placed under a 1 m² cardboard sheet where 33 × 33 square cells were drawn: cells size is $\Delta x = \Delta y = 3$ cm (for clarity, in Fig. 6 the reader is shown on the top of the sheet). In Fig. 6, the

reader electronic board appears as an external device, even though it is commonly accommodated inside the desktop reader case. In Fig. 7, the RSSI distribution is shown for the LABID UH414 tag with orientation parallel to *x*-axis and *y*-axis, on the entire test area. For each cell, the RSSI value has been obtained by averaging the RSSI samples collected in a 10 s interval. Similar distributions can be obtained for the tag read rate. When the *modular antenna configuration* is employed, the tag can be read at any position and orientation on the reader surface (Figs. 7*a* and *b*). Also, there are no false positives if the tagged item is located at more than 10–15 cm from the case edge. The average read rate on the antenna area is around 8 tag/s. Reading performance is worse at the lower edge of the desktop reader, where free space is available to accommodate the reader electronic circuit. By using the *spiral TWA configuration*, the tag is read when it lies directly above the antenna central area (Figs. 7*c* and *d*). By approaching the antenna borders, the tag detection fails, so successfully avoiding false positives. For both tag orientations, an average read rate of 8 tag/s has been measured in a detection area of about 4 × 5 cells (12 cm × 15 cm). To measure the reader antenna read range, further tests have been carried out by moving the tag away from the antenna surface, with a step of 5 cm. At each distance, the RSSI value has been averaged in an interval of 10 s, for two orthogonal tag orientations. The read range (Fig. 8) is around 60 and 10 cm for the *modular antenna configuration* and the *spiral TWA configuration*, respectively, regardless of the tag orientation. A value of −90 dBm has been associated to missed readings. Writing tests have also been performed, as such operation requires higher field amplitudes with respect to the tag reading operation. Results in terms of writing attempts are shown in Fig. 9. The area in which the *modular antenna configuration* allows writing operations (with one or two attempts) is extended up to their borders. On the contrary, the *spiral TWA configuration* allows a successful writing operation with just one attempt in a limited area in the antenna centre and this is desirable to avoid tag initialisation outside the antenna surface.

3.2 Multiple tags detection

Finally, 11 LABID UH414 tags have been placed in a stacked configuration at a distance of 2 cm from each other, up to an overall height of 20 cm (tags are separated by a foam layer), as shown in Fig. 6*c*. The lower tag has been placed directly on the case surface. The stacked tags readability has been tested on a surface subdivided into 9 × 5 cells (cells sizes are $\Delta x = \Delta y = 3$ cm). The total number of tags detected in a 10 s time interval has been recorded, when varying the tag orientation and the stack position on the antenna surface. Results are shown in Fig. 10. When using the modular antenna (Figs. 10*a* and *b*), almost all the 11 stacked tags are read in each cell of the antenna surface, for both orthogonal tag orientations. As for single-tag tests, performance get worse at the desktop reader lower border, where free space is available to accommodate the reader electronic circuit. Besides, the *spiral TWA configuration* is able to detect just an average number of five tags, with a maximum number of seven tags at the antenna centre, regardless of tag orientation (Figs. 10*c* and *d*). This was expected due to its rapid field spatial decay.

Similar considerations apply to the read rate distributions. Indeed,
a high read rate has been observed for the modular antenna configuration: 111 tag/s and 100 tag/s for the *x*-oriented tag and *y*-oriented tag, respectively. For the *spiral TWA configuration*, the average read rate on the whole antenna surface reduces to 32 tag/s and 27 tag/s for the *x*-oriented tag and *y*-oriented tag, respectively.

Above test measurements confirm that the modular antenna represents a low-cost solution that allows to select the best shape and size of the NF reader detection volume, as a function of both the operation required (reading or writing) and the number of the tagged items that the operator is going to put on the reader surface.

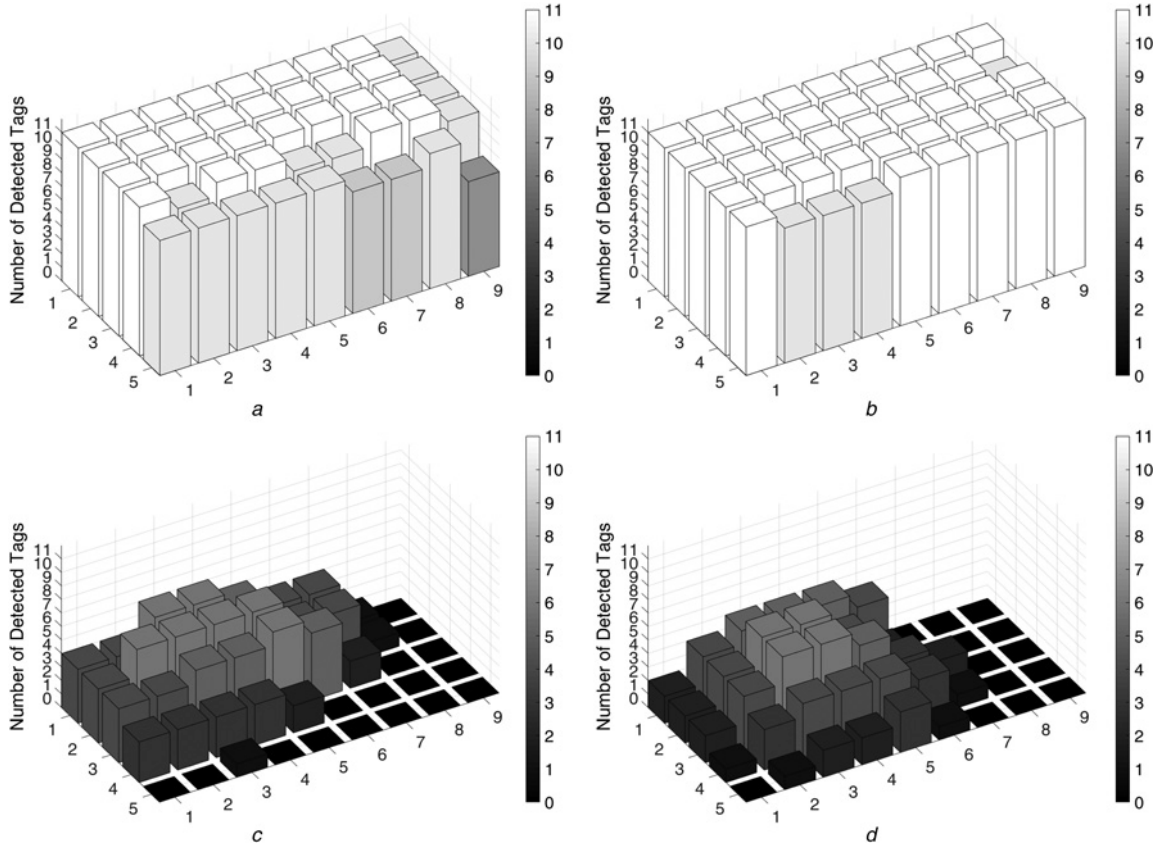

Fig. 10 *Number of detected tags on the antenna surface by employing 11 LABID UH414 stacked tags at a distance of 2 cm each other, up to a height of 20 cm (the first tag has been placed directly in contact with the surface of the antenna)*
a Modular antenna at *x*-oriented UH414 *b* Modular antenna at *y*-oriented UH414 *c* Spiral TWA at *x*-oriented UH414
d Spiral TWA at *y*-oriented UH414

4 Conclusion

A multifunctional modular antenna for NF UHF RFID desktop readers has been designed and tested. It operates at the FCC band and can fit into a reader case whose size is around 30 cm × 18 cm × 1.5 cm. In the proposed layout, a spiral-shaped TWA is positioned at the centre of the reader surface. By means of a switch, the spiral can be connected to either an array of two miniaturised CP patches or a matched load. When the spiral TWA is ended on the matched load, the reader detection volume is limited to a small area at the centre of the reader surface. The latter configuration being preferred during writing operations, namely when the only tag to be encoded is most likely placed at the antenna centre, or when tagged items are read one at a time. Conversely, if the power at the output of the spiral microstrip is used to feed the array (instead of being absorbed by the matched load), the two-module antenna exhibits a lower rate of the field spatial decay when moving away from the centre of the reader surface. The latter feature is of interest when reading of stacked tags is required.

It has to be underlined that by simply adjusting the length of the TWA (the latter being a non-resonating antenna) the proposed modular antenna can fit in reader cases with shape and size that are different from those considered here by the authors. Indeed, the antenna scalability is an important feature when designing low-profile NF antennas for RFID-based smart storage spaces (such as drawers and shelves).

5 Acknowledgments

The authors acknowledge CAEN RFID s.r.l. (Viareggio, Lucca, Italy) for the technical support and for providing the measurement setup. They also acknowledge the support of CST for providing additional resources and technical assistance for the parallel version of CST Microwave Studio®.

6 References

1 Buffi, A., Nepa, P., Lombardini, F.: ‘A phase-based technique for localization of UHF-RFID tags moving on a conveyor belt: performance analysis and test-case measurements’, *IEEE Sens. J.*, 2015, 15, (1), pp. 387–396

2 Buffi, A., Nepa, P.: ‘A phase-based technique for discriminating tagged items moving through a UHF-RFID gate’. 2014 IEEE RFID Technology and Applications Conf. (RFID-TA), 2014, pp. 155–158

3 Buffi, A., Serra, A.A., Nepa, P., *et al.*: ‘A focused planar microstrip array for 2.4 GHz RFID readers’, *IEEE Trans. Antennas Propag.*, 2010, 58, (5), pp. 1536–1544

4 Kalansuriya, P., Bhattacharyya, R., Sarma, S.: ‘RFID tag antenna-based sensing for pervasive surface crack detection’, *IEEE Sens. J.*, 2013, 13, (5), pp. 1564–1570

5 Shao, S., Burkholder, R.J.: ‘Item-level RFID tag location sensing utilizing reader antenna spatial diversity’, *IEEE Sens. J.*, 2013, 13, (10), pp. 3767–3774

6 Catarinucci, L., Colella, R., Mainetti, L., *et al.*: ‘Smart RFID antenna system for indoor tracking and behavior analysis of small animals in colony cages’, *IEEE Sens. J.*, 2014, 14, (4), pp. 1198–1206

7 Michel, A., Buffi, A., Caso, R., *et al.*: ‘Design and performance analysis of a planar antenna for near-field UHF-RFID desktop readers’. Asia-Pacific Microwave Conf. Proc. (APMC), 2012, pp. 1019–1021

8 Michel, A., Caso, R., Buffi, A., *et al.*: ‘Meandered TWAS array for near-field UHF RFID applications’, *Electron. Lett.*, 2014, 50, (1), pp. 17–18

9 Caso, R., Michel, A., Buffi, A., *et al.*: ‘A modular antenna for UHF RFID near-field desktop reader’. IEEE RFID Technology and Applications Conf. (RFID-TA), 2014, pp. 204–207

10 Michel, A., Buffi, A., Caso, R., *et al.*: ‘A scalable modular antenna configuration to extend the detection volume of a near-field UHF-RFID desktop reader’. IEEE Int. Symp. on Antennas and Propagation & USNC/URSI National Radio Science Meeting, 19–24 July 2015, pp. 1766–1767

11 Michel, A., Buffi, A., Caso, R., *et al.*: ‘A two-element modular antenna for near-field UHF RFID applications’. 1st URSI Atlantic Radio Science Conf. (URSI AT-RASC), 2015, 16–24 May 2015, pp. 1–1

12 Michel, A., Buffi, A., Nepa, P., *et al.*: ‘Antennas for UHF-RFID printer-encoders’. IEEE 15th Mediterranean Microwave Symp. (MMS), 30 November 2015–2 December 2015, pp. 1–4

13 Medeiros, C.R., Costa, J.R., Fernandes, C.A.: ‘RFID reader antennas for tag detection in self-confined volumes at UHF’, *IEEE Antennas Propag. Mag.*, 2011, 53, (2), pp. 39–50

14 Andrenko, A.S., Kai, M.: ‘Novel design of UHF RFID near-field antenna for smart shelf applications’. Asia-Pacific Microwave Conf. Proc. (APMC), 2013, pp. 242–244

15 Hong, J., Choo, J., Ryoo, J., *et al.*: ‘A shelf antenna using near-field without dead zones in UHF RFID’. ICIT 2009 IEEE Int. Conf. on Industrial Technology, 2009, pp. 1–4

16 Dobkin, D.M., Weigand, S.M., Iye, N.: ‘Segmented magnetic antennas for near-field UHF RFID’, *Microw. J.*, 2007

17 Qing, X., Goh, C.K., Chen, Z.N.: ‘A broadband UHF near-field RFID antenna’, *IEEE Trans. Antennas Propag.*, 2010, 58, (12), pp. 3829–3838

18 Ren, A., Wu, C., Gao, Y., *et al.*: ‘A robust UHF near-field RFID reader antenna’, *IEEE Trans. Antennas Propag.*, 2012, 60, (4), pp. 1690–1697

19 Yuan, Y., Yu, D.: ‘UHF RFID shelf solution with cascaded reader antenna and positioning capability’. IEEE Int. Conf. on RFID, 2012

20 Michel, A., Caso, R., Buffi, A., *et al.*: ‘An array of meander travelling wave antennas for near-field UHF-RFID readers’. IEEE Antennas and Propagation Society Int. Symp. (APSURSI), 2013, pp. 1732–1733

21 Choi, W., Kim, J.-S., Bae, J.-H., *et al.*: ‘Near-field antenna for a radio frequency identification shelf in the uhf band’, *IET Microw. Antennas Propag.*, 2010, 4, (10), pp. 1538–1542

22 Cho, C., Ryoo, J., Park, I., *et al.*: ‘Design of a novel ultra-high frequency radio-frequency identification reader antenna for near-field communications using oppositely directed currents’, *IET Microw. Antennas Propag.*, 2010, 4, (10), pp. 1543–1548

23 Ding, X., Wu, Q., Zhang, K., *et al.*: ‘A magnetic coupling dipole for UHF near-field RFID reader’, *IEEE Trans. Magn.*, 2012, 48, (11), pp. 4305–4308

24 Michel, A., Nepa, P.: ‘UHF-RFID desktop reader antennas: performance analysis in the near-field region’, *IEEE Antennas Wirel. Propag. Lett.*, 2015, to appear

25 Michel, A., Caso, R., Buffi, A., *et al.*: ‘Modular antenna for reactive and radiative near-field regions of UHF-RFID desktop readers’. XXXIth URSI General Assembly and Scientific Symp. (URSI GASS), 2014, pp. 1–4

26 Bertocco, M., Dalla Chiara, A.D., Sona, A.: ‘Performance evaluation and optimization of UHF RFID systems’. IEEE Instrumentation and Measurement Technology Conf. (I2MTC), 2010, pp. 1175–1180

27 Kolundzija, B.M., Mrdakovic, B.L.: ‘Analysis of space coverage in far field UHF RFID systems’. Int. Workshop on Antenna Technology (iWAT), 2010, pp. 1–4
28 Buffi, A., Michel, A., Caso, R., *et al*.: ‘Near-field coupling in UHF-RFID systems’. Proc. of URSI Int. Symp. on Electromagnetic Theory (EMTS), 2013, pp. 408–411
29 Buffi, A., Nepa, P., Manara, G.: ‘Analysis of near-field coupling in UHF-RFID systems’. IEEE-APS Topical Conf. on Antennas and Propagation in Wireless Communications (APWC), 2011, pp. 931–934
30 Chen, Y.-S., Chen, S.-Y.: ‘Analysis of antenna coupling in near-field RFID systems’. IEEE Antennas and Propagation Society Int. Symp. (APSURSI), 2009, pp. 1–4
31 Fuschini, F., Piersanti, C., Sydanheimo, L., *et al*.: ‘Electromagnetic analyses of near field UHF RFID systems’, *IEEE Trans. Antennas Propag.*, 2010, 58, (5), pp. 1759–1770
32 de Souza, A.C., Duroc, Y., Vuong, T.P., *et al*.: ‘Quantitative evaluation of power transfer efficiency of UHF RFID passive systems’, *Electron. Lett.*, 2015, 51, (12), pp. 932–933
33 de Souza, A.C., Vuong, T.P., Duroc, Y., *et al*.: ‘Normalized power calculation to UHF RFID passive tags characterization’. IEEE Brasil RFID, 2014, pp. 54–56
34 Caso, R., Michel, A., Rodriguez-Pino, M., *et al*.: ‘Dual-band UHF-RFID/WLAN circularly polarized antenna for portable RFID readers’, *IEEE Trans. Antennas Propag.*, 2014, 62, (5), pp. 2822–2826
35 Guraliuc, A.R., Buffi, A., Caso, R., *et al*.: ‘Axial ratio analysis of single-feed circularly polarized resonant antennas’, *J. Electromagn. Waves Appl.*, 2014, 28, (6), pp. 716–728
36 http://www.caenrfid.it/en/
37 http://www.lab-id.com/datasheet/inlay_UHF/UH414.pdf